PNAS NEXUS

PNAS Nexus, 2025, 4, pgaf077
https://doi.org/10.1093/pnasnexus/pgaf077
Advance access publication 3 March 2025
Research Report

Medial ganglionic eminence transplantation restores inhibition after central visual system brain injury

Bowen Hou[a,b], Jisu Eom[a,b], David C. Lyon[a,b,c] and Robert F. Hunt[a,b,d,*]

[a]Department of Anatomy & Neurobiology, UCI School of Medicine, Med. Sci. B, Room 240, Irvine, CA 92697, USA
[b]Epilepsy Research Center, University of California, 847 Health Sciences Quad, Irvine, CA 92467, USA
[c]Center for Translational Vision Research, University of California, 829 Health Sciences Rd, Irvine, CA 92617, USA
[d]Sue and Bill Gross Stem Cell Research Center, University of California, 845 Health Sciences Rd, Irvine, CA 92697, USA
*To whom correspondence should be addressed: Email: robert.hunt@uci.edu
Edited By Eric Klann

Abstract

Inhibitory interneurons are critical regulators of visual circuit function and plasticity, but they are partially lost after brain injury. It has been hypothesized that embryonic medial ganglionic eminence (MGE) progenitors transplanted into visual cortex may facilitate brain repair, but there is no evidence that MGE cells modify inhibition in the damaged visual system. Here, we demonstrate that MGE progenitors transplanted into primary visual cortex of adult mice with traumatic brain injury (TBI) migrate widely throughout the lesioned area and express molecular markers of mature inhibitory interneurons. Whole-cell voltage-clamp recordings of inhibitory postsynaptic currents obtained from layer 2/3 host neurons, 45–60 days after transplantation, revealed a significant loss of GABA-mediated synaptic inhibition after TBI. Following MGE transplantation, we found significant increases in synaptic inhibition in regions of visual cortex containing transplanted MGE progenitors. Our results therefore provide direct evidence that MGE transplantation enhances local inhibition after central visual system brain injury.

Keywords: synaptic inhibition, interneuron, vision, traumatic brain injury, cell therapy

Significance Statement

Inhibitory progenitors derived from the mouse embryonic medial ganglionic eminence can migrate, integrate, and increase inhibition following transplantation into the juvenile or adult brain. However, in primary visual cortex, transplanted inhibitory neurons are proposed to form weak connections with nearby excitatory neurons, exerting their effects indirectly through parabiosis rather than fully integrating into the host network. This study provides compelling evidence that inhibitory neuron transplantation enhances synaptic inhibition in visual cortex of a mouse model of central visual system injury. These observations not only reinforce restored synaptic inhibition as the primary cellular mechanism of brain repair by interneuron transplantation but also enhance our understanding of inhibitory circuit plasticity in the damaged visual system.

Introduction

Transplantation of inhibitory neurons from the embryonic medial ganglionic eminence (MGE) has emerged as a reliable strategy to regenerate interneurons in the damaged or diseased brain. When grafted from embryos, MGE progenitors migrate long distances, integrate into host networks as physiologically mature parvalbumin (PV) and somatostatin (SST) interneuron subtypes, and selectively enhance GABAergic neurotransmission onto host principal neurons (1–8). The therapeutic efficacy of this approach was first demonstrated in mouse models of epilepsy (3, 5), which often involve a loss or dysfunction of inhibitory neurons (9–11). This was followed by a robust literature documenting successful therapeutic results in related disorders where a loss of inhibition is a major contributor, such as Alzheimer's disease (6, 12), stroke (13), traumatic brain injury (TBI) (8), intellectual disability (14), Parkinson's disease (4), neuropathic pain (15), and psychosis (16). In all cases, the cellular properties of transplanted interneurons were found to closely resemble their native-born counterparts.

Several independent studies have demonstrated a robust ability of MGE cells to incorporate structurally and functionally into the juvenile or adult brain. Transplanted MGE progenitors form synaptic contacts locally onto host principal neurons, as documented by electron microscopy ultrastructural analysis (3), and they receive orthotopic local and long-range input from across the brain, as documented by rabies circuit mapping analysis (17, 18). Using paired patch-clamp recordings or optogenetic

Competing Interest: The authors declare no competing interests.
Received: August 16, 2024. **Accepted:** February 8, 2025
© The Author(s) 2025. Published by Oxford University Press on behalf of National Academy of Sciences. This is an Open Access article distributed under the terms of the Creative Commons Attribution-NonCommercial-NoDerivs licence (https://creativecommons.org/licenses/by-nc-nd/4.0/), which permits non-commercial reproduction and distribution of the work, in any medium, provided the original work is not altered or transformed in any way, and that the work is properly cited. For commercial re-use, please contact reprints@oup.com for reprints and translation rights for reprints. All other permissions can be obtained through our RightsLink service via the Permissions link on the article page on our site—for further information please contact journals.permissions@oup.com.

photostimulations, several groups have independently documented strong synaptic connections between transplanted and host neurons, consistent with the interneuron subtypes being regenerated (19–22). When MGE-grafted cells are silenced, through DREADD-inactivation (8) or VGAT loss-of-function (23), the therapeutic effects of transplantation are not observed or are reversed. Collectively, these studies provide relatively direct evidence that the beneficial effects of MGE cell transplantation are driven by the precise structural and electrophysiological integration of new interneurons into host networks.

Surprisingly, in primary visual cortex (V1), it has been proposed that MGE progenitors work indirectly by releasing parabiosis-like rejuvenating factors that modify host brain circuits rather than fully integrating into the host network (24, 25). This alternate view raises the question of whether interneuron loss, or MGE transplantation, would have the same effect on GABA-mediated inhibition in V1 as seen in other areas of the central nervous system. We have shown previously that mild TBI to V1 produces a long-lasting reduction of interneuron density and impairments in V1 neuron orientation and size tuning, which are mediated through local cortical inhibition (26). Here, we tested the effect of TBI on synaptic inhibition in V1 and whether MGE transplantation could restore inhibition, as we have demonstrated following TBI to hippocampus (8).

Results

MGE transplantation produces new GABA neurons in brain-injured V1

The potential for MGE progenitors to migrate, differentiate, and integrate following transplantation is influenced by the host brain environment (27, 28). We therefore first tested whether brain-injured visual cortex would permit the widespread incorporation of transplanted MGE progenitors. To do this, we performed a mild unilateral controlled cortical impact (CCI) injury centered over V1 in young adult male mice at P60 (0.2 mm impact depth, 3.5 ms^{-1}, and 500 ms duration; Fig. 1A). We selected CCI injury because it produces a highly reproducible focal contusion injury, one of the most common types of posterior impact injury observed in human (29). We harvested MGE progenitors from E13.5 β-actin:GFP donor mice to allow for their visualization after transplantation (30). Then, 7 days after the brain injury, we made one injection of 3×10^4 MGE cells into ipsilateral V1 at the site of injury (i.e. the injury epicenter).

In all brain-injured animals ($n = 19$ mice), the lesion consisted of mild tissue compression at the injury epicenter in V1 (Fig. 1B and C). The injury site was marked by an intense immunostaining for glial fibrillary acidic protein (GFAP) ipsilateral to the injury (contralateral: 4.7 ± 0.8%, ipsilateral: 8.4 ± 0.9%; $P = 2.15E{-}04$; two-tailed paired t test; $n = 3$ mice; Fig. 1B); ionizing calcium-binding adaptor molecule 1 (IBA1) was not elevated at this time point (contralateral: 6.1 ± 0.7%, ipsilateral: 7.3 ± 0.9%; $P = 0.23$; two-tailed paired t test; $n = 3$ mice). This pattern of cortical damage matched our previous time-course characterization of glial responses after mild TBI to V1 (26). At 30 days after transplantation (DAT), MGE-grafted cells dispersed up to 1,200 µm rostral–caudal from the injection site (Fig. 1C–E) and occupied all layers of the lesioned visual cortex ($n = 3$ mice). However, GFP + cells largely remained localized to injured V1, defined as the area of GFAP immunostaining in neocortex. Survival of transplanted MGE cells was 6.5 ± 1.3% ($n = 3$ mice), which is more robust than prior studies transplanting MGE into adult naive control neocortex (28) but less than brain-injured hippocampus (8). GFP-labeled cells were rarely found outside of V1 and never found outside neocortex. This observation is similar to the columnar distribution that has been reported of MGE cell grafts into adult control neocortex (28). Transplanted cells had morphological features of mature GABAergic interneurons, with large, extensive arborizations that covered the full extent of brain-injured V1.

To characterize the molecular identity of transplanted MGE cells, we immunostained coronal sections of recipient V1 at 30 DAT for GFP and known markers of GABAergic interneurons (Fig. 2). The majority of GFP-labeled cells expressed GAD67 (84.9 ± 0.4%), and colabeled cells expressed the interneuron makers SST (28.6 ± 2.6%) and PV (17.4 ± 4.5%) at levels consistent with prior MGE transplantation studies (5, 8, 28). Few GFP + cells expressed vasoactive intestinal peptide (VIP; 2.9 ± 1.6%), which labels a population of GABAergic neurons that originate from the caudal ganglionic eminence (19). GFP + cells did not colabel with GFAP (0%, $n = 3$ animals) or IBA1 (0%, $n = 3$ animals). These results show transplanted MGE progenitors survive, migrate, and differentiate into subtypes of GABAergic interneurons in brain-injured V1 with molecular identities that are consistent with the developmental origin of MGE cells.

Synaptic inhibition is reduced after TBI and increased by MGE transplantation

There are fewer inhibitory neurons in V1 after TBI (26), but it is unclear whether there are long-term changes in synaptic inhibition to V1 neurons. Furthermore, whether MGE progenitors have meaningful functional effects on synaptic inhibition in host V1 has never been tested. We therefore assessed the overall level of synaptic inhibition in brain-injured animals with and without MGE cell grafts by measuring inhibitory postsynaptic currents (IPSCs) onto layer 2/3 pyramidal neurons in V1 45–60 DAT (Fig. 3A). Regions of V1 containing GFP + cells were identified under epifluorescence (Fig. 3B), and V1 pyramidal neurons at the injury site surrounded by GFP + cells were chosen for patch-clamp recordings. Similar locations were chosen in acute brain slices from control and brain-injured mice that did not receive MGE cells.

Spontaneous (i.e. network-driven) IPSCs were recorded at a holding potential of −70 mV in the presence of 1 mM kynurenic acid to block glutamate receptors. V1 neurons from brain-injured mice showed a 60% decrease in sIPSC frequency compared with age-matched controls ($n = 12$ cells from five control mice, $n = 9$ cells from four TBI mice) (Fig. 3B and C). In slices from MGE-grafted mice containing GFP + cells, sIPSC frequency was restored to control levels ($n = 11$ cells from five TBI–MGE mice) (Fig. 3D). No change in event amplitude was detected among the groups (control: 31.0 ± 2.1 pA, V1-TBI: 44.3 ± 6.2 pA, V1-TBI + MGE: 39.0 ± 4.4 pA; one-way ANOVA, $F_{(2, 29)} = 2.48$, $P = 0.1$) (Fig. 3E). Likewise, no difference was detected in sIPSC 10–90% rise time (control: 0.73 ± 0.08 ms, V1-TBI: 0.61 ± 0.07 ms, V1-TBI + MGE: 0.54 ± 0.05 ms; one-way ANOVA, $F_{(2, 29)} = 2.09$, $P = 0.14$) or decay time constant (control: 5.82 ± 0.84 ms, V1-TBI: 6.45 ± 0.83 ms, V1-TBI + MGE: 5.40 ± 0.36 ms; one-way ANOVA, $F_{(2, 29)} = 0.51$, $P = 0.61$).

Miniature (i.e. action potential–independent) IPSCs were recorded in the presence of 1 mM kynurenic acid and 1 µM TTX in some of the same slices used to examine spontaneous activity (Fig. 4A). Similar to spontaneous events, mIPSC frequency was significantly decreased by ~45% in V1 neurons at the injury site and significantly increased 45–60 days after MGE transplantation (Fig. 4B). Differences in mIPSC amplitude were not detected between the groups (Fig. 4C). Likewise, no difference was detected in mIPSC 10–90% rise time (control: 0.76 ± 0.11 ms, V1-TBI: 0.57 ± 0.06 ms, V1-TBI +

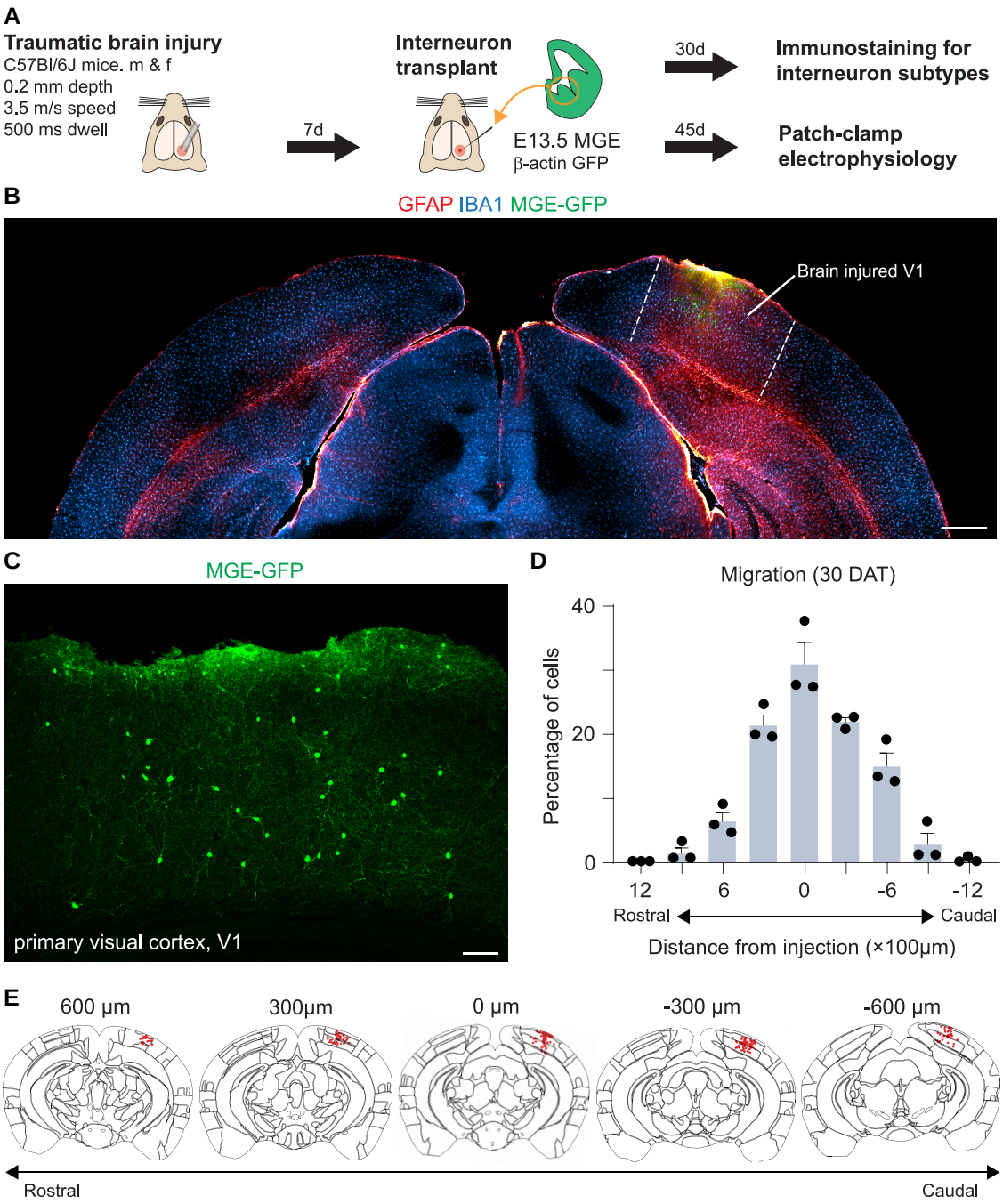

Fig. 1. Transplanted MGE cells migrate into brain-injured visual cortex. A) Schematic of experimental design. B and C) Coronal slice of CCI-injured V1 30 DAT labeled for GFAP (red), IBA1 (blue), and GFP + transplanted neurons (green). MGE cells dispersed throughout all layers of injured V1. D) Distribution of transplanted MGE cells 30 DAT ($n = 3$ mice). E) Schematic coronal sections (50 μm) showing individual MGE cells registered in standardized atlas space. One red dot represents one neuron.

MGE: 0.55 ± 0.05 ms; one-way ANOVA, $F_{(2, 29)} = 2.4$, $P = 0.11$) or decay time constant (control: 5.9 ± 1.06 ms, V1-TBI: 5.6 ± 0.46 ms, V1-TBI + MGE: 5.34 ± 0.38 ms; one-way ANOVA, $F_{(2, 29)} = 0.2$, $P = 0.82$). Taken together, these results demonstrate a robust integration of transplanted GABA neurons leading to a substantial enhancement of synaptic inhibition in brain-injured V1.

Discussion

TBI produces long-lasting reductions in GABAergic neurons (31–38) and a marked loss of inhibition within injured areas of the brain (36, 37, 39–42). However, V1 has a remarkable degree of plasticity that allows the visual system to adapt to dynamic environments, and the effect of TBI on synaptic inhibition in V1 has never been tested. Using a mouse model of focal central visual system neurotrauma, we found that a mild contusive injury to V1 in adulthood leads to a long-lasting decrease in synaptic inhibition onto layer 2/3 principal neurons. These results are consistent with previous reports documenting a loss of inhibitory neurons using the same injury parameters (26). We further show MGE transplantation into brain-injured visual cortex, which does not normally add new neurons throughout life, produced new

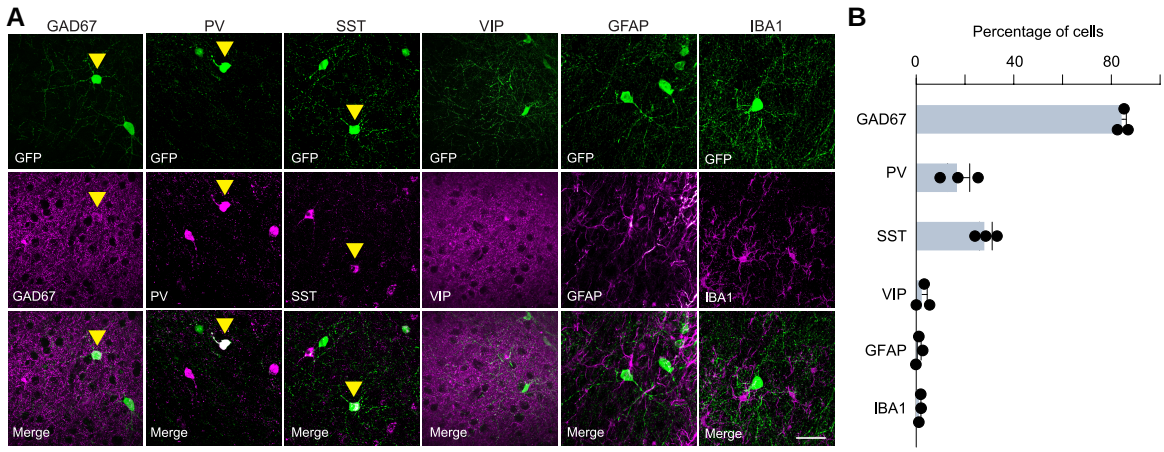

Fig. 2. Transplanted MGE cells express markers of inhibitory neurons. A) Representative confocal images in V1 (30 DAT) of immunostaining for GFP (green) and molecular markers of inhibitory neurons and glial cell types (magenta). Arrowheads, colabeled cells; scale bars, 25 μm. B) Quantification of marker expression of GFP-labeled cells in brain-injured animals at 30 DAT ($n = 3$ mice per marker). PV, parvalbumin; SST, somatostatin; VIP, vasoactive intestinal peptide; GFAP, glial fibrillary acidic protein; IBA1, ionizing calcium-binding adaptor molecule 1.

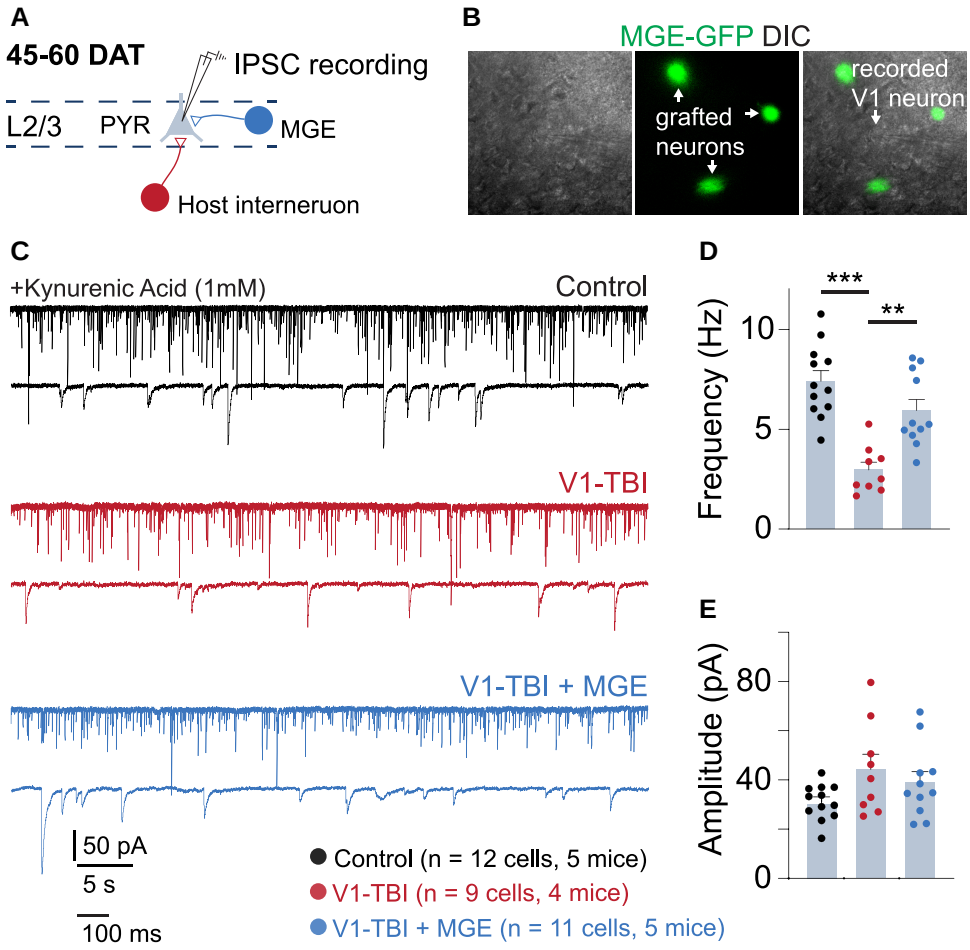

Fig. 3. MGE transplantation increases network-driven inhibition after central visual system TBI. A) Schematic of the patch-clamp protocol. B) Acute coronal slice of V1 with GFP$^+$ cells in layer 2/3 visualized under IR-DIC and epifluorescence. A recording was obtained from a pyramidal neuron in the vicinity of GFP$^+$ cells (white arrows). C) Representative patch-clamp recordings of sIPSCs from V1 neurons in a control (black), a brain-injured mouse injected with media (V1-TBI, red), or a brain-injured mouse implanted with MGE cells (V1-TBI + MGE, blue). Recordings were obtained from slices 45–60 DAT. D) Quantification of sIPSC frequency. ***$P = 4.37E{-}06$, control vs V1-TBI; **$P = 1.32E{-}03$, V1-TBI vs V1-TBI + MGE; one-way ANOVA with Bonferroni's post hoc test. $n = 12$ cells from five control mice, 9 cells from four V1-TBI mice, and 11 cells from five V1-TBI + MGE mice. E) Quantification of sIPSC amplitude.

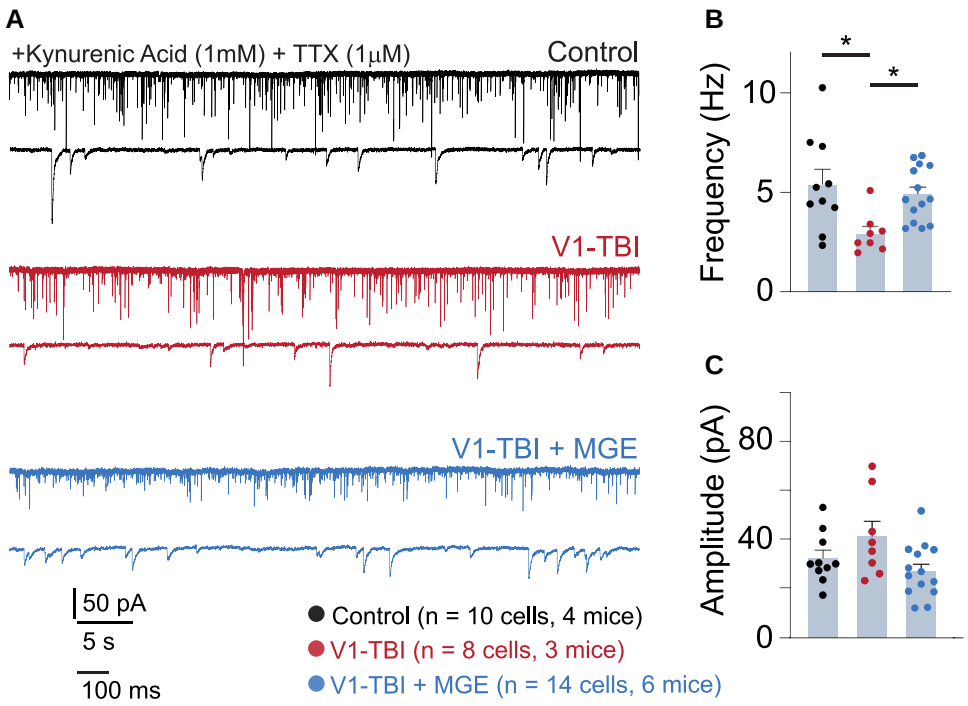

Fig. 4. MGE transplantation increases synaptic inhibition after central visual system TBI. A) Representative patch-clamp recordings of mIPSCs from V1 neurons in a control (black), a brain-injured mouse injected with media (V1-TBI, red), or a brain-injured mouse implanted with MGE cells (V1-TBI + MGE, blue). Recordings were obtained from slices 45–60 DAT. B) Quantification of mIPSC frequency. *P =1.4E−02, control vs V1-TBI; *P = 4.2E−02, V1-TBI vs V1-TBI + MGE; one-way ANOVA with Bonferroni's post hoc test. *n* = 10 cells from four control mice, 8 cells from three V1-TBI mice, and 14 cells from six V1-TBI + MGE mice. C) Quantification of mIPSC amplitude.

GABAergic neurons, and restored synaptic inhibition to levels that were indistinguishable from controls. This is consistent with results obtained from hippocampus in rodent models of epilepsy (3, 5), Alzheimer's disease (6), and TBI (8) and in control animals (2).

Our results are not surprising, because they are consistent with a robust literature supporting the structural and functional integration of transplanted MGE cells into host brain networks (1–8, 12, 15, 17–22). Nevertheless, they counter a prevailing idea that, in V1, transplanted interneurons may not integrate properly and therefore only play an indirect role in modifying circuit plasticity (24, 25). While our results cannot directly rule out additional parabiosis-like effects of MGE cells, as has been speculated by prior studies (24), our findings support the general idea that transplanted MGE cells enhance GABAergic inhibition locally onto host principal neurons as has been documented in every other area of the central nervous system. We found MGE cell survival to be robust in brain-injured V1, compared with prior transplants into neocortex of naïve adult animals (28). It is possible that MGE survival is enhanced in an injured brain due to interneuron cell loss or some other factor that facilitates inhibitory progenitor cell survival.

Permanent visual dysfunction is an extremely common health burden of individuals and military service members living with TBI (29, 43, 44). In V1, inhibitory neuron activity is critical for basic visual circuit properties, such tuning a neuron's preference for stimulus contrast, size, and orientation (45–48), and higher-order processing, such as contrast perception (49). Following TBI, V1 neurons show broader orientation tuning and spatial summation (26), which is consistent with visual dysfunction related, at least in part, to reduced inhibitory neuron activity (47). Based on the slice electrophysiology results observed here, and our recent success using interneuron transplantation to treat posttraumatic memory problems and epilepsy (8, 18), future studies evaluating MGE transplantation into V1 may reveal a new therapeutic approach to correct such posttraumatic visual circuit dysfunctions.

Materials and methods

Animals

Male and female C57BL/6J mice (Jackson Laboratories, cat. no. 000664) were maintained in standard housing conditions on a 12-h light/dark cycle with food and water provided ad libitum. Embryonic donor tissue was produced by crossing wild-type CD1 mice (Charles River Laboratories, cat. no. 022) to homozygous β-actin EGFP mice (Jax stock no. 006567) maintained on a CD1 background. All protocols and procedures were first approved by and followed the guidelines of the University Laboratory Animal Resources at the University of California, Irvine, and adhered to the National Institutes of Health Guidelines for the Care and Use of Laboratory Animals. All CCI-specific common data elements defined by PRE Clinical Interagency reSearch resourcE—TBI (PRECISE-TBI) are given in Table S1.

Experimental design

Upon arrival, animals were habituated to their housing for up to 1 week before being coded and randomly assigned into uninjured (naive control), media-injected (V1-TBI), or MGE-injected (V1-TBI + MGE) treatment groups. Brain-injured mice and age-matched controls were housed together (2–5 animals per cage). The order of injury and cell transplantation was also randomized. For all experiments, animals from each treatment group were examined together (i.e. experiments were never staggered in time)

and performed in a randomized order by an investigator blinded to treatment. Experiments were not blinded, because injured animals could be clearly identified by the craniotomy and GFP epifluorescence was used to select cells for patch-clamp recordings.

Brain injury

Unilateral CCI was performed at P60 as previously described (8, 26). Briefly, mice were first anesthetized with 2% isoflurane until they were unresponsive to toe-pinch. The fur overlying the skull was then trimmed, and mice were placed into a stereotactic frame and maintained on 1 to 1.5% isoflurane. The scalp was gently cleaned with betadine before exposing the skull with a midline incision. To target V1 for injury, the skull was rotated 20° counterclockwise along the rostral–caudal axis and the rostral end of the skull was lowered 20° relative to skull flat. This orientation centered the impactor tip at the rostral end of V1. A 4- to 5-mm craniotomy was made 3 mm lateral to midline and 3 mm rostral to the lambdoid suture in the right hemisphere. The skull cap was removed leaving the dura intact. A computer-controlled, pneumatically driven impactor (TBI-0310, Precision Systems and Instrumentation) with a 3-mm beveled stainless steel tip was used to deliver a contusive injury perpendicular to the dura at 0.2 mm depth, 3.5 m/s velocity, and 500 ms dwell time. The skull cap was not replaced, and the incision was closed with silk sutures. Animals undergoing surgical procedures received buprenorphine hydrochloride (Buprenex, 0.05 mg/kg, delivered i.p.) preoperatively and once daily for 3 days. A postoperative health assessment was performed daily for 5 days following surgical procedures and periodically until the day of experimentation.

MGE transplantation

Ventricular and subventricular layers of the MGE were harvested from E13.5 GFP + embryos. The time point at which the sperm plug was detected was considered E0.5. Embryonic MGE explants were dissected in Leibovitz L-15 medium, mechanically dissociated by repeated pipetting in L-15 medium, and concentrated by centrifugation (3 min at $600 \times g$). Concentrated cell suspensions were front loaded into beveled glass micropipettes (50 μm tip diameter, Wiretol 5 μL, Drummond Scientific) and injected (3×10^4 cells in a single injection) into V1 of adult brain-injured mice 7 days after CCI injury. We chose 7 days post-TBI as the time for transplantation based on prior work showing a 1-week delay between lesion and transplantation an optimal clinically relevant therapeutic time window for transplanting cells in models of TBI (8). Target coordinates were first verified in a series of preliminary dye injection studies into control and brain-injured mice (Fig. S1). Cell injections were made into V1 at the following stereotaxic coordinates: anterior–posterior (AP) −3.25 mm, medial–lateral 2.25 mm, and dorsal–ventral 0.8 mm. Brain-injured controls were injected with an equal volume of L-15 media at each site. Cell viability (>85%) and concentration were quantified using 0.5 μL of the cell suspension mixed with 24.5 μL of L-15 medium and 25 μL of trypan blue (Sigma) (8).

Immunostaining

Mice were transcardially perfused with 4% paraformaldehyde, and free-floating vibratome sections (50 μm) were processed using standard immunostaining procedures (8). Sections were stained with the following primary antibodies: GFP (1:1,000; cat. no. GFP-1020, Aves Labs), GAD67 (1:1,000; cat. no. MAB5406, Millipore), PV (cat. no. P3088, Millipore), SST (1:500; cat. no. MAB354, Millipore), VIP (1:500; cat. no. 20077, Immunostar), GFAP (1:500; cat. no. MAB3402, Millipore), and IBA1 (1:1,000, cat. no. 019-19740, Fujifilm). Secondary antibodies were Alexa 488, 546, and 647 (1:1,000; cat. nos. A-11039, A-11030, A-11035, A-11007, and A-21244, Fisher Scientific). Sections were then mounted on charged slides (Superfrost Plus; Fisher Scientific) with Fluoromount-G containing DAPI (Southern Biotech). Images were obtained with a Leica DM6 epifluorescence microscope. Confocal images were obtained with an Olympus FV3000 or a Zeiss 900 laser scanning microscope. Brightness and contrast were adjusted manually using ImageJ; z-stacks were generated using Olympus or Zeiss software.

Cell quantification

Fluorescently labeled coronal brain sections (50 μm) were imaged using a Leica DM6 fluorescence microscope with an × 20 objective, and quantification was performed using ImageJ, as previously described (8). All cells that expressed GFP and/or a subtype marker were counted in every sixth coronal section through the entire brain (that is, 300 μm apart). All sections containing grafted cells were analyzed per animal and the values averaged to obtain a mean cell density (cells/mm^2). For quantification of GFAP and IBA1 immunostaining, measurements were analyzed at three different locations and the percentage of area above fluorescence threshold was applied using ImageJ according to a previous protocol (8). The same settings were used for all sections.

Slice preparation

Mice were rapidly anesthetized by isoflurane inhalation, as previously described (50). While deeply anesthetized, mice were decapitated, the brain was extracted and placed in ice-cold (2–4°C) oxygenated high-sucrose artificial CSF (ACSF) containing the following (in mm): 150 sucrose, 50 NaCl, 25 $NaHCO_3$, 10 dextrose, 2.5 KCl, 1 NaH_2PO_4-H_2O, 0.5 $CaCl_2$, and 7 $MgCl_2$, pH 7.2–7.4 (equilibrated with 95% O_2–5% CO_2, 300–305 mOsm/kg). After 1 to 2 min, the brain was glued to a metal plate, and coronal brain slices (300 μm thick) were prepared from V1 45–60 DAT in ice-cold, oxygenated high-sucrose ACSF using a Vibratome (Leica VTS1000). Slices were transferred to a storage chamber containing oxygenated ACSF containing the following (in mm): 124 mM NaCl, 3 mM KCl, 1.25 mM NaH_2PO_4-H_2O, 2 mM $MgSO_4$-7 H_2O, 26 mM $NaHCO_3$, 10 mM dextrose, and 2 mM $CaCl_2$ (pH 7.2–7.4, 300–305 mOsm kg^{-1}) and maintained at room temperature until used for experimentation.

Slice electrophysiology

After an equilibration period of at least 60 min, slices were submerged in the recording chamber and continuously perfused with oxygenated ACSF (32–34°C). Whole-cell patch-clamp recordings were performed at × 40 using an upright, fixed-stage microscope (Olympus BX50WI) equipped with infrared differential interference contrast and epifluorescence optics. Layer 2/3 V1 neurons were identified morphologically within the slice as having pyramidal somata with visible apical dendrites, as done in prior work (51). For voltage-clamp recordings of IPSCs, patch pipettes (2–4 MΩ) were pulled from borosilicate glass (1.5 mm outer diameter and 0.45 mm wall thickness; World Precision Instruments) with a P-1000 puller (Sutter Instruments). The internal solution contained the following (in mM): 140 CsCl, 11 EGTA, 10 HEPES, 1 $MgCl_2$, 2 NaATP, and 0.5 NaGTP (pH 7.22, 292 mOsm kg^{-1}). Recordings were obtained with a Multiclamp 700B amplifier, filtered at 10 kHz, and recorded to pClamp 11.2 software (Clampfit; Molecular Devices). After membrane rupture, cells were first

voltage clamped for ~5 min at −70 mV to allow equilibration of intracellular and recording pipette contents. Voltage-clamp recordings were then examined at a holding potential of −70 mV, and GABAergic currents were measured in the presence of 1 mM kynurenic acid (Sigma-Aldrich, K3375). Tetrodotoxin (TTX, 1 μM) was added to the ACSF to record miniature events. Bicuculline (30 uM) was applied to confirm events are driven by postsynaptic $GABA_A$ receptors (Fig. S2). Series resistance was typically <15 MΩ and was monitored throughout the recordings. Data were only used for analysis if the series resistance remained <20 MΩ and changed by ≤20% during the recordings. Recordings were not corrected for a liquid junction potential. In MGE-grafted animals, recordings were only performed in slices in which GFP + cells could be visually identified.

Quantification and statistical analysis

Data quantification and analyses were performed using ImageJ, Easy Electrophysiology, and GraphPad Prism 8 software. A 1-min sample recording per cell was used for measuring synaptic event frequency, amplitude, and kinetics. Events characterized by a typical fast rising phase and exponential decay phase were manually detected using Easy Electrophysiology. Only currents with amplitudes greater than three times the root mean square noise level were included for analysis. Event frequency, mean amplitude, and kinetics were averaged across neurons (i.e. n = neurons), and groups were compared by one-way ANOVA for multiple comparisons with Bonferroni's post hoc test when appropriate. Shapiro–Wilk test did not show a significant departure from normality for any comparison. Kinetic analysis of the IPSCs was performed with a single-exponential function for 10–90% rise time and a biexponential function to calculate decay time constant. Sample sizes were determined based on previous MGE transplantation studies (5, 8). Data are expressed as mean ± SEM, and significance was set at $P < 0.05$.

Acknowledgments

The authors thank members of the Hunt Lab for helpful discussions and comments during the preparation of this manuscript.

Supplementary Material

Supplementary material is available at *PNAS Nexus* online.

Funding

This work was supported by funding from the Department of Defense grant W81XWH-21-1-0884 to R.F.H. and D.C.L., California Institute for Regenerative Medicine Research Scholar Award EDUC4-12822 to B.H., and National Institutes of Health grant R01-NS096012 to R.F.H.

Author Contributions

R.F.H. and D.C.L. were involved in conceptualization. B.H., J.E., and R.F.H. contributed to methodology and investigation. R.F.H. and D.C.L. were involved in supervision. R.F.H. was involved in writing—original draft. B.H., J.E., D.C.L., and R.F.H. were involved in review and editing.

Data Availability

All data are included in the manuscript.

References

1 Wichterle H, Garcia-Verdugo JM, Herrera DG, Alvarez-Buylla A. 1999. Young neurons from medial ganglionic eminence disperse in adult and embryonic brain. *Nat Neurosci*. 2:461–466.
2 Alvarez-Dolado M, *et al*. 2006. Cortical inhibition modified by embryonic neural precursors grafted into the postnatal brain. *J Neurosci*. 26:7380–7389.
3 Baraban SC, *et al*. 2009. Reduction of seizures by transplantation of cortical GABAergic interneuron precursors into Kv1.1 mutant mice. *Proc Natl Acad Sci U S A*. 106:15472–15477.
4 Martínez-Cerdeño V, *et al*. 2010. Embryonic MGE precursor cells grafted into adult rat striatum integrate and ameliorate motor symptoms in 6-OHDA-lesioned rats. *Cell Stem Cell*. 6:238–250.
5 Hunt RF, Girskis KM, Rubenstein JL, Alvarez-Buylla A, Baraban SC. 2013. GABA progenitors grafted into the adult epileptic brain control seizures and abnormal behavior. *Nat Neurosci*. 16:692–697.
6 Tong LM, *et al*. 2014. Inihibitory interneuron progenitor transplantation restores normal learning and memory in ApoE4 knock-in mice without or with Ab accumulation. *J Neurosci*. 34:9506–9515.
7 Casalia ML, Howard MA, Baraban SC. 2017. Persistent seizure control in epileptic mice transplanted with gamma-aminobutyric acid progenitors. *Ann Neurol*. 82:530–542.
8 Zhu B, Eom J, Hunt RF. 2019. Transplanted interneurons improve memory precision after traumatic brain injury. *Nat Commun*. 10:5156.
9 de Lanerolle NC, Kim JH, Robbins RJ, Spencer DD. 1989. Hippocampal interneuron loss and plasticity in human temporal lobe epilepsy. *Brain Res*. 495:387–395.
10 Kobayashi M, Buckmaster PS. 2003. Reduced inhibition of dentate granule cells in a model of temporal lobe epilepsy. *J Neurosci*. 23:2440–2452.
11 Cobos I, *et al*. 2005. Mice lacking Dlx1 show subtype-specific loss of interneurons, reduced inhibition and epilepsy. *Nat Neurosci*. 8:1059–1068.
12 Martinez-Losa M, *et al*. 2018. Nav1.1-overexpressing interneuron transplants restore brain rhythms and cognition in a mouse model of Alzheimer's disease. *Neuron*. 98:75–89.e5.
13 Daadi MM, *et al*. 2009. Functional engraftment of the medial ganglionic eminence cells in experimental stroke model. *Cell Transplant*. 18:815–826.
14 Kim YJ, *et al*. 2018. Chd2 is necessary for neural circuit development and long-term memory. *Neuron*. 100:1180–1193.
15 Bráz JM, *et al*. 2012. Forebrain GABAergic neuron precursors integrate into adult spinal cord and reduce injury-induced neuropathic pain. *Neuron*. 74:663–675.
16 Gilani AI, *et al*. 2014. Interneuron precursor transplants in adult hippocampus reverse psychosis-relevant features in a mouse model of hippocampal disinhibition. *Proc Natl Acad Sci U S A*. 111:7450–7455.
17 Juarez-Salinas DL, *et al*. 2019. GABAergic cell transplants in the anterior cingulate cortex reduce neuropathic pain aversiveness. *Brain*. 142:2655–5669.
18 Frankowski JC, Tierno A, *et al*. 2022. Brain-wide reconstruction of inhibitory circuits after traumatic brain injury. *Nat Commun*. 13:3417.
19 Larimer P, *et al*. 2016. Caudal ganglionic eminence precursor transplants disperse and integrate as lineage-specific interneurons but do not induce cortical plasticity. *Cell Rep*. 16:1391–1404.

20 Howard MA, Baraban SC. 2016. Synaptic integration of transplanted interneuron progenitor cells into native cortical networks. *J Neurophysiol*. 116:472–478.

21 Hsieh JY, Baraban SC. 2017. Medial ganglionic eminence progenitors transplanted into hippocampus integrate in a functional and subtype-appropriate manner. *eNeuro*. 4:ENEURO.0359-16.2017.

22 Larimer P, Spatazza J, Stryker MP, Alvarez-Buylla A, Hasenstaub AR. 2017. Caudal ganglionic eminence precursor transplants disperse and integrate as lineage-specific interneurons but do not induce cortical plasticity. *J Neurophysiol*. 18:131–139.

23 Priya R, *et al*. 2019. Vesicular GABA transporter is necessary for transplant-induced critical period plasticity in mouse visual cortex. *J Neurosci*. 39:2635–2648.

24 Zheng X, *et al*. 2021. Host interneurons mediate plasticity reactivated by embryonic inhibitory cell transplantation in mouse visual cortex. *Nat Commun*. 12:862.

25 Southwell DG, Froemke RC, Alvarez-Buylla A, Stryker MP, Gandhi SP. 2010. Cortical plasticity induced by inhibitory neuron transplantation. *Science*. 327:1145–1148.

26 Frankowski JC, *et al*. 2021. Traumatic brain injury to primary visual cortex produces long-lasting circuit dysfunction. *Commun Biol*. 4:1297.

27 Quattrocolo G, Fishell G, Petros TJ. 2017. Heterotopic transplantations reveal environmental influences on interneuron diversity and maturation. *Cell Rep*. 21:721–731.

28 Paterno R, Vu T, Hsieh C, Baraban SC. 2024. Host brain environmental influences on transplanted medial ganglionic eminence progenitors. *Sci Rep*. 14:3610.

29 Armstrong RA. 2018. Visual problems associated with traumatic brain injury. *Clin Exp Optom*. 101:716–726.

30 Hadjantonakis A, Gertenstein M, Ikawa M, Okabe M, Nagy A. 1998. Generating green fluorescent mice by germline transmission of green fluorescent ES cells. *Mech Dev*. 76:79–90.

31 Lowenstein DH, Thomas MJ, Smith DH, McIntosh TK. 1992. Selective vulnerability of dentate hilar neurons following traumatic brain injury: a potential mechanistic link between head trauma and disorders of the hippocampus. *J Neurosci*. 12:4846–4853.

32 Toth Z, Hollrigel GS, Gorcs T, Soltesz I. 1997. Instantaneous perturbation of dentate interneuronal networks by a pressure wave-transient delivered to the neocortex. *J Neurosci*. 17:8106–8117.

33 Santhakumar V, *et al*. 2000. Granule cell hyperexcitability in the early post-traumatic rat dentate gyrus: the 'irritable mossy cell' hypothesis. *J Physiol*. 524(Pt 1):117–134.

34 Gupta A, Elgammal FS, Proddutur A, Shah S, Santhakumar V. 2012. Decrease in tonic inhibition contributes to increase in dentate semilunar granule cell excitability after brain injury. *J Neurosci*. 32:2523–2537.

35 Cantu D, *et al*. 2015. Traumatic brain injury increases cortical glutamate network activity by compromising GABAergic control. *Cereb Cortex*. 25:2306–2320.

36 Butler CR, Boychuk JA, Smith BN. 2016. Differential effects of rapamycin treatment on tonic and phasic GABAergic inhibition in dentate granule cells after focal brain injury in mice. *Exp Neurol*. 280:30–40.

37 Nichols J, Bjorklund GR, Newbern J, Anderson T. 2018. Parvalbumin fast-spiking interneurons are selectively altered by paediatric traumatic brain injury. *J Physiol*. 596:1277–1293.

38 Frankowski JC, Kim YJ, Hunt RF. 2019. Selective vulnerability of hippocampal interneurons to graded traumatic brain injury. *Neurobiol Dis*. 129:208–216.

39 Li H, Prince DA. 2002. Synaptic activity in chronically injured, epileptogenic sensory-motor neocortex. *J Neurophysiol*. 88:2–12.

40 Hunt RF, Scheff SW, Smith BN. 2011. Synaptic reorganization of inhibitory hilar interneuron circuitry after traumatic brain injury in mice. *J Neurosci*. 31:6880–6890.

41 Pavlov I, *et al*. 2011. Progressive loss of phasic, but not tonic, GABAA receptor-mediated inhibition in dentate granule cells in a model of post-traumatic epilepsy in rats. *Neuroscience*. 194:208–219.

42 Almeida-Suhett CP, *et al*. 2015. GABAergic interneuronal loss and reduced inhibitory synaptic transmission in the hippocampal CA1 region after mild traumatic brain injury. *Exp Neurol*. 273:11–23.

43 Sano K, Nakamura N, Hirakawa K, Masuzawa H, Hashizume K. 1967. Mechanism and dynamics of closed head injuries (preliminary report). *Neurol Med Chir (Tokyo)*. 9:21–33.

44 Stelmack JA, Frith T, Van Koevering D, Rinne S, Stelmack TR. 2009. Visual function in patients followed at a Veterans Affairs polytrauma network site: an electronic medical record review. *Optometry*. 80:419–424.

45 Sillito AM, Salt TE, Kemp JA. 1985. Modulatory and inhibitory processes in the visual cortex. *Vision Res*. 25:375–381.

46 Cardin JA, Palmer LA, Contreras D. 2007. Stimulus feature selectivity in excitatory and inhibitory neurons in primary visual cortex. *J Neurosci*. 27:10333–10344.

47 Lee SH, *et al*. 2012. Activation of specific interneurons improves V1 feature selectivity and visual perception. *Nature*. 488:379–383.

48 Liu YJ, Hashemi-Nezhad M, Lyon DC. 2015. Contrast invariance of orientation tuning in cat primary visual cortex neurons depends on stimulus size. *J Physiol*. 593:4485–4498.

49 Cone JJ, Scantlen MD, Histed MH, Maunsell JHR. 2019. Differe`nt inhibitory interneuron cell classes make distinct contributions to visual contrast perception. *eNeuro*. 6:ENEURO.0337-18.2019.

50 Hunt RF, Dinday MT, Hindle-Katel W, Baraban SC. 2012. LIS1 deficiency promotes dysfunctional synaptic integration of granule cells generated in the developing and adult dentate gyrus. *J Neurosci*. 32:12862–12875.

51 Stanco A, *et al*. 2014. NPAS1 represses the generation of specific subtypes of cortical interneurons. *Neuron*. 84:940–953.